Diagn Interv Radiol 2012; 18:27–33

ABDOMINAL IMAGING

ORIGINAL ARTICLE

Evaluation of CT as a predictor for kidney and renal artery mobility

Paul Guzzetta, Piotr Obara, Abraham Dachman

PURPOSE

Renal artery stent failure may result from excessive kidney mobility in some patients. We used computed tomography (CT) to determine the prevalence and magnitude of renal displacement due to postural changes.

MATERIALS AND METHODS

A retrospective review of 100 consecutive CT colonography examinations was performed to measure renal artery location and displacement in both axial and coronal views using paired supine and prone non-contrast scans. Kidney displacement from the prone to supine position was correlated with a change in renal artery angular deviation. Statistical significance was determined using *t*-tests and Pearson correlations. Results were based on measurements made by a single observer.

RESULTS

Mobility and angular displacement between the prone and supine positions were significant bilaterally and in both planes ($P < 0.01$) except for the coronal plane kidney mobility on the left ($P = 0.32$). The axial plane correlation between kidney and artery mobility was significant bilaterally (left/right R=0.44/0.22, $P < 0.01$/0.03); the coronal plane correlation was only significant on the left (left/right R=0.26/0.18, P = 0.01/0.08). The mean axial plane mobility and angle change were greater on the left (left/right mobility 13 mm/7 mm; left/right angle change 18°/8°). In contrast, the mean coronal plane mobility and angle change were greater on the right (left/right mobility 4 mm/22 mm; left/right angle change 4°/8°). Fourteen patients had a mobility in excess of 32°.

CONCLUSION

During postural changes, the kidneys and renal arteries demonstrate significant correlated mobility. Renal artery movements can be identified using a low-radiation dose CT exam.

Key words: • *CT colonography* • *renal artery obstruction* • *atherosclerosis*

Vascular stenting is a non-invasive method often used to treat patients with renal artery stenosis (1). Stent failure or restenosis is reported to occur in approximately 17% of patients (0%–40%) (2–5). Multiple factors can contribute to renal artery stent failure or restenosis (6). One of these factors is thought to be kidney mobility and renal artery mobility leading to stent fracture (7–11). Increased artery mobility has been found to be associated with stent fracture in other sites, namely the iliac arteries, superficial femoral arteries, and bile ducts (12–14). Although data regarding the clinical importance of renal artery stent fracture are lacking, significant restenosis is correlated with fracture in other sites and may be as high as 67% and 76% in the femoropopliteal and superficial femoral arteries, respectively (15, 16).

The movement of a stent within a mobile artery exacerbates the risk of stent restenosis and thrombosis in addition to the risk of stent fracture (17). Restenosis is most commonly the result of stent-induced endothelial trauma leading to an exaggerated repair process, inflammation and intimal hyperplasia (18–23). Similarly, thrombosis results from the exposure of thrombogenic arterial wall components after endothelial injury (24). In addition to intimal hyperplasia, chronic stent recoil has been shown to account for some lumen loss in stented renal arteries (25). The additional shear stress caused by a mobile artery may potentially accelerate stent recoil and restenosis and increase the risk of thrombus formation (17, 26).

Kidney and renal artery mobility are likely factors in stent failure and restenosis, and establishing mobility preoperatively may be clinically useful in predicting future failure. Knowledge about the magnitude of renal artery and stent movements may also be useful in designing and testing new stents. Kidney position and the renal artery angle have been shown to change with inspiration and expiration (27–29). Body position changes have also been shown to alter cardiovascular and renal physiology (30–33). However, no data exist on the range of kidney or renal artery mobility with changes in body position. Additionally, the magnitude of renal artery movement required to cause stent malfunction is unknown.

To evaluate the ability of computed tomography (CT) to identify kidney and renal artery mobility, we retrospectively compared supine and prone images from a cohort of CT colonography patients and measured the changes in kidney location and renal artery angle. We also correlated the degree of kidney mobility to the change in renal artery angle.

Materials and methods

Patients

All patients undergoing CT colonography consented to participation in this research study. The scans of 100 consecutive patients were analyzed; the patient population included 51 males and 49 females, with

From the Department of Radiology (P.O. ✉ *probara@gmail.com*), University of Chicago Medical Center, Chicago, IL, USA.

Received 4 November 2010; revision requested 10 January 2011; revision received 15 February 2011; accepted 16 February 2011.

Published online 31 May 2011
DOI 10.4261/1305-3825.DIR.4049-10.1

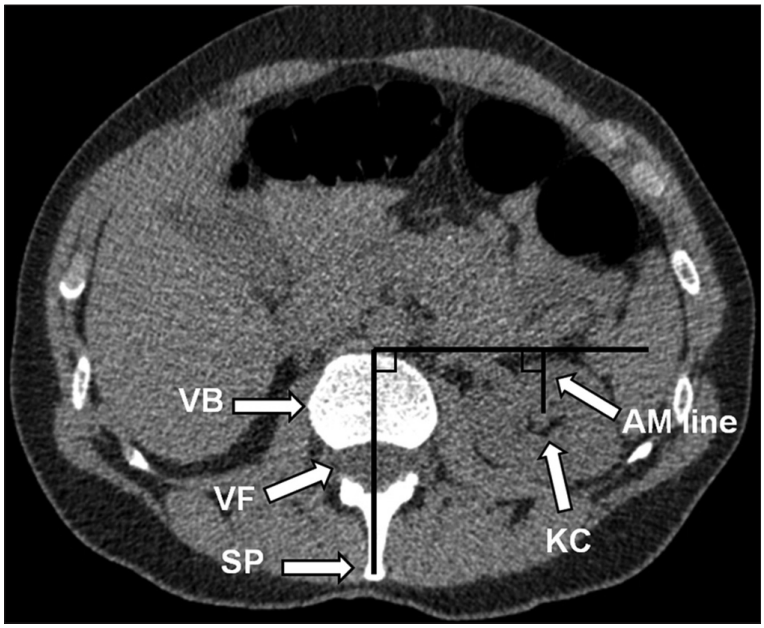

Figure 1. Method to determine kidney mobility in the anteroposterior direction. Axial slice at the level of the center of the right kidney. A line is drawn from the spinal process through the middle of the vertebral foramen to the anterior crest of the vertebral body. Another line is drawn from the anterior crest of the vertebral body at a 90° angle to the first line. The second line serves as a reference landmark from which the anterior or posterior movement of the kidney is measured. A third line extending from this landmark at a 90° angle is drawn to the center of the kidney. The change in the length of this line between the supine and the prone views is the metric used for the kidney mobility in the axial plane (axial mobility line). The initial measurement is obtained in the prone view and subtracted from the measurement in the supine view, which typically yields a positive number. VB, vertebral body; VF, vertebral foramen; SP, spinal process; KC, kidney center; AM line, axial mobility line.

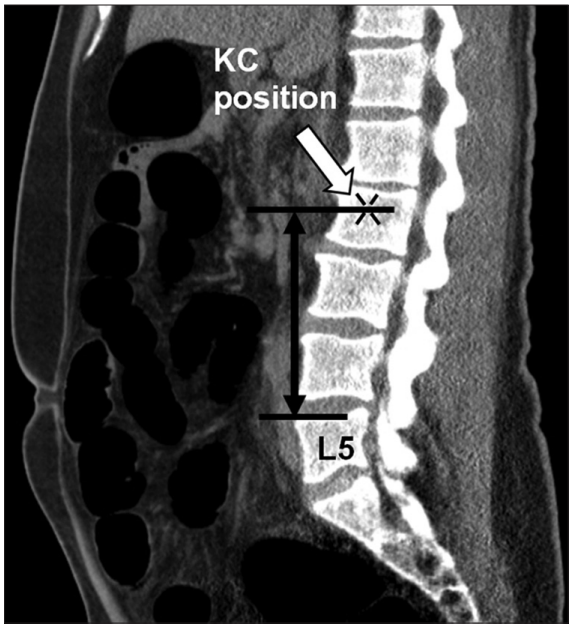

Figure 2. Method to determine kidney mobility in the cephalocaudal direction. Sagittal slice at the hemi-section of the vertebral body. The center of the kidney is located using all three planes and marked with an X. The marked X is then correlated to the sagittal plane. The sagittal images are used to locate the anterior-cephalic corner of the L5 vertebral body, which serves as a reference landmark. A line is drawn from the anterior-cephalic corner of L5 vertically to the same horizontal level as the center of the kidney. This line is measured in both the prone and supine views. The initial measurement is obtained in the prone view and subtracted from the measurement in the supine view; which typically yields a positive number. KC, kidney center.

a mean age of 61 years (range, 42–95 years). No patients with known conditions that would have allowed for unusually increased organ or vascular mobility were included in this study.

Image acquisition

CT colonography exams were performed on a 64-slice scanner (Philips Brilliance, Philips Healthcare, Andover, Massachusetts, USA) using a 40×0.625 detector configuration, a 0.5 s rotation time, 50 mAs/slice, 120 kVp (140 kVp for obese patients), and the filter "B" algorithm; the reconstruction was based on 1 mm thick slices at 0.8 mm intervals. All exams were done without intravenous contrast enhancement using a standard breath-hold protocol after maximal inspiration. Patients were scanned in both the supine and prone positions. The CT datasets were transferred to a workstation (GE Advantage Windows Workstation ver. 4.2-06; GE Healthcare Global Diagnostic Imaging Inc., Waukesha, Wisconsin, USA) and viewed in the CT colonography package. Three-dimensional multiplanar reformats were generated for all patients undergoing CT colonography. The workstation software allows viewing of any oblique plane for both the supine and prone views with pixel-to-pixel correlation between multi-planar views. Linear measurements can be made in any plane. The images were viewed in a standard soft tissue window (window=400, level=40).

Kidney mobility measurement

The anteroposterior and cephalocaudad displacement of the kidneys was measured based on the change in location of the center of the kidney between prone and supine views. The center of the kidney was visually approximated in all three planes and marked. The change in the kidney position was then determined by measuring the distance between the kidney center and a vertebral landmark reference point in both the supine and prone positions. Multi-planar reconstructions were viewed in 10 mm thick reconstructions. The method of measuring anteroposterior mobility of the kidney as seen in the axial plane is described in Fig. 1. The method of measuring the cephalocaudal mobility of the kidney as seen in the sagittal plane is described in Fig. 2.

Renal artery angle measurement

The axial slice at the level of origin of the superior mesenteric artery (SMA) was selected. To compensate for the variable tortuosity and position of the aorta, a line connecting the center of the aorta and the SMA origin was drawn (Fig. 3a). While the aorta-SMA line position varied from patient to patient due to the variable SMA origin, this line remained constant in each patient when changing postures from supine to prone. Therefore, this aorta-SMA line served as a supine-prone reference point from which to measure the postural change in the axial plane renal artery angle. The origin of the renal artery was identified on both sides in all cases. The method of measuring

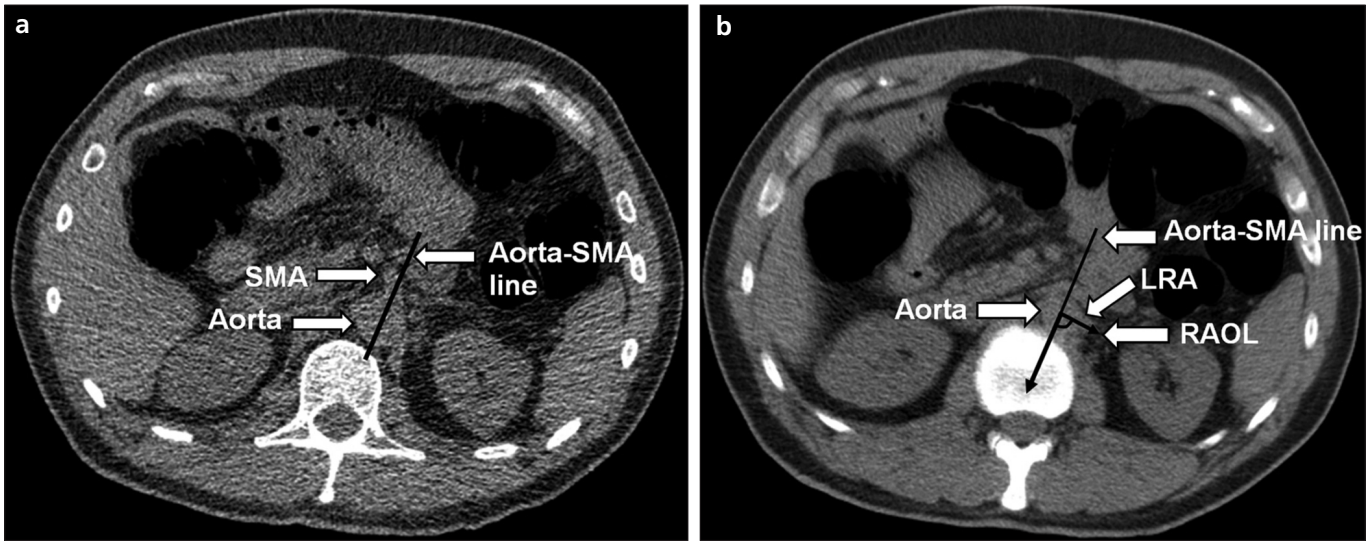

Figure 3. a, b. Method to determine the axial renal artery origin angles. **(a)** Axial image at the level of the superior mesenteric artery. A line connecting the center of the aorta and the superior mesenteric artery origin is drawn to create an Aortic-SMA line. **(b)** Axial slice at the level of the renal artery origin. The Aorta-SMA line is drawn on this view using precisely the same orientation. A line from the first few millimeters of the renal artery (bold line) is extended to the Aorta-SMA line. This is called the renal artery origin line. The angle that results between the renal origin line and the Aortic-SMA line is measured. SMA, Superior mesenteric artery; LRA, left renal artery; RAOL, renal artery origin line.

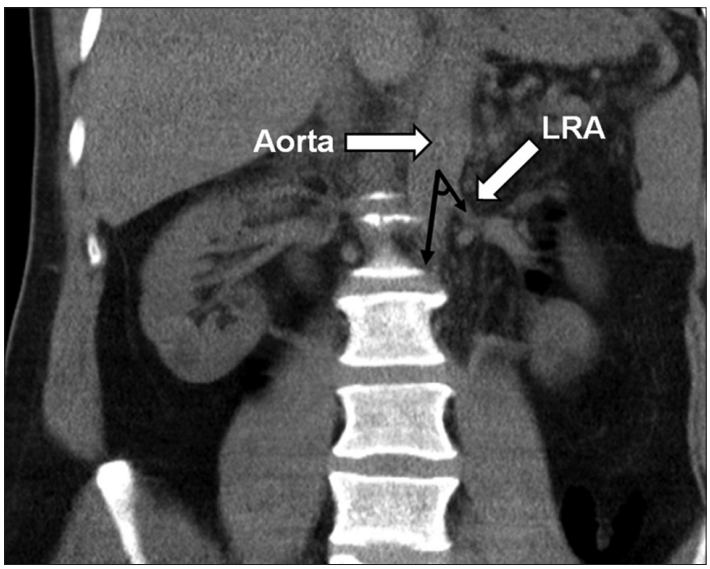

Figure 4. Diagram showing method to determine the right renal artery origin angle in the coronal plane. Coronal slice at the level of the center of the renal artery origin. A line is drawn parallel to the axis of the aorta at the level of the renal artery origin as viewed on a 10 mm thick reconstruction. Using a 2 mm reconstruction, a line from the first few millimeters of the renal artery to the line of the aortic axis is drawn. The resulting aorta to renal artery angle is measured. LRA, Left renal artery.

the renal artery angle change as seen in the axial plane is shown in Fig. 3b. The method of measuring the renal artery angle change as seen in the coronal plane is described in Fig. 4. The measurements were performed independently for the main right and left renal arteries. Accessory vessels were not included.

Data analysis

Results were based on a single medical student's measurements (observer #1). In addition, observer #1 and another medical student (observer #2) each performed two sets of measurements on a random sample of ten consecutive patients to determine intra- and inter-observer variability. Observers underwent a detailed tutorial from an experienced supervising radiologist on how to take kidney mobility measurements; however, they did not have prior experience interpreting abdominal images. Data were analyzed separately for the right and left kidneys, for the axial and coronal planes, and for the supine and prone positions. We calculated the difference in the renal artery angles and the kidney movement between the two body positions and evaluated each for statistically significant changes using a paired *t*-test. Statistical significance only indicates that there was a measurable difference in the renal position and renal artery angle with a postural change and does not imply clinical significance. A *t*-test was also used to determine any differences in the angle change and kidney mobility between males and females. For each patient, changes in the angle were plotted against the corresponding kidney mobility to generate a scatter plot. A trend line was interpolated from the scatter plot, and the data were subjected to a Pearson correlation test to determine the statistical significance of the relationship. Pearson correlation was also used to determine the relationship of renal artery movement between the right and left sides and between the axial and coronal planes on the same side.

To approximate an angle change that could potentially have a clinically significant risk, the mean and standard deviation of the absolute magnitude of all angle changes (i.e., in both axial and coronal planes and on both sides) were calculated. The absolute value of the angle changes were chosen for

this calculation because the magnitude of movement, and not the direction, would be of greater clinical significance and because the absolute value data could be more easily utilized in future studies of mobility. Angle change values of one standard deviation and two standard deviations above the mean were arbitrarily chosen as thresholds that could potentially pose a clinically significant risk for stent malfunction, and the number of patients with movement above each of these angle thresholds was determined. Extreme angle change was defined as greater than two standard deviations above the average.

The concordance correlation coefficient (CCC) and Pearson correlation coefficient (*r*) were used to assess intra- and inter-observer agreement in measuring the renal artery angle change and kidney mobility (34, 35). The average value of each observer's two measurements was used for inter-observer analysis. The study was conducted with approval of the institutional review board.

Results

Kidney mobility

The prone to supine kidney position changes were averaged for both kidneys and for both anteroposterior and cephalocaudal directions of movement (Table 1). Movement of the kidney with body position change from prone to supine was statistically significant in both directions on the right and only in the anteroposterior direction on the left ($P < 0.01$; Fig. 5a and 5b). The cephalocaudal left kidney movement was not statistically significant on average ($P = 0.29$); there was a significant difference in females (mean mobility, 5.5 mm; range, -27.7 to 32.1 mm; $P < 0.01$) but not in males (mean mobility, -2.1 mm; range, -44.2 to 37 mm; $P = 0.73$). Anteroposterior mobility was greater on the left; however, cephalocaudal plane mobility was greater on the right (Table 1).

Renal artery angle change

The left and right renal artery ostium angle changes were averaged for both the axial and coronal views (Table 2). With the change in body position, the renal artery angle changed significantly on both sides and in both planes ($P < 0.01$; Fig. 5c and 5d). The greatest angle change was seen on the left side in the

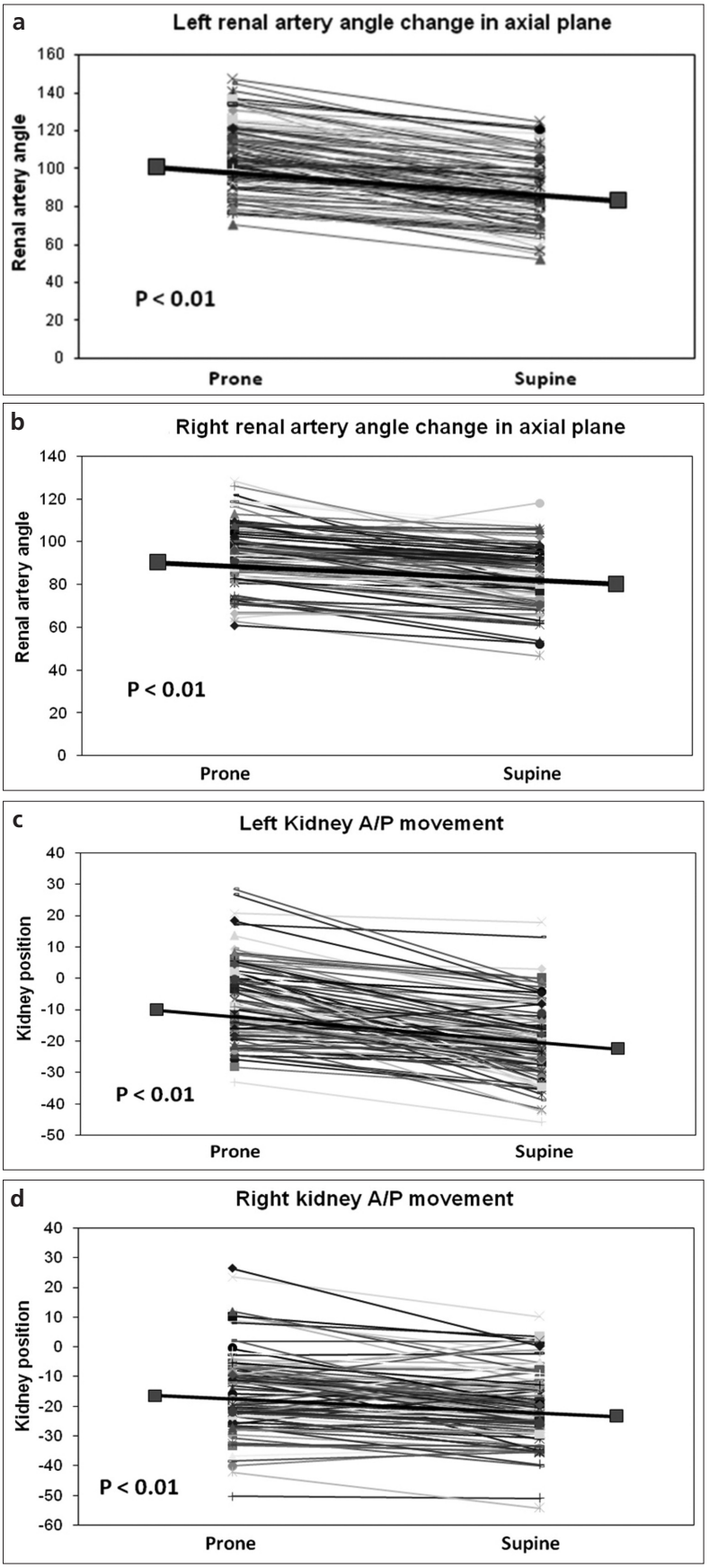

Figure 5. a–d. Changes in the renal artery angle **(a, b)** and the kidney position **(c, d)** with prone to supine patient movement. Data points on the longer line represent mean values. A/P, anteroposterior.

Table 1. Renal mobility (n=100 patients)

		Position in prone (mm)	Position in supine (mm)	Change in position (Prone–supine) (mm)
Axial plane[a]				
	Left kidney	7	21	13 (range, -1 to 49) $P < 0.01$
	Right kidney	15	21	7 (range, -4 to 32) $P < 0.01$
Coronal plane[b]				
	Left kidney	119	114	4 (range, -44 to 37) $P = 0.29$
	Right kidney	131	109	22 (range, -16 to 63) $P < 0.01$

[a]Antero-posterior kidney mobility.
[b]Cephalo-caudal kidney mobility.
Kidney center determined in coronal plane; distance from landmark measured in sagittal plane.

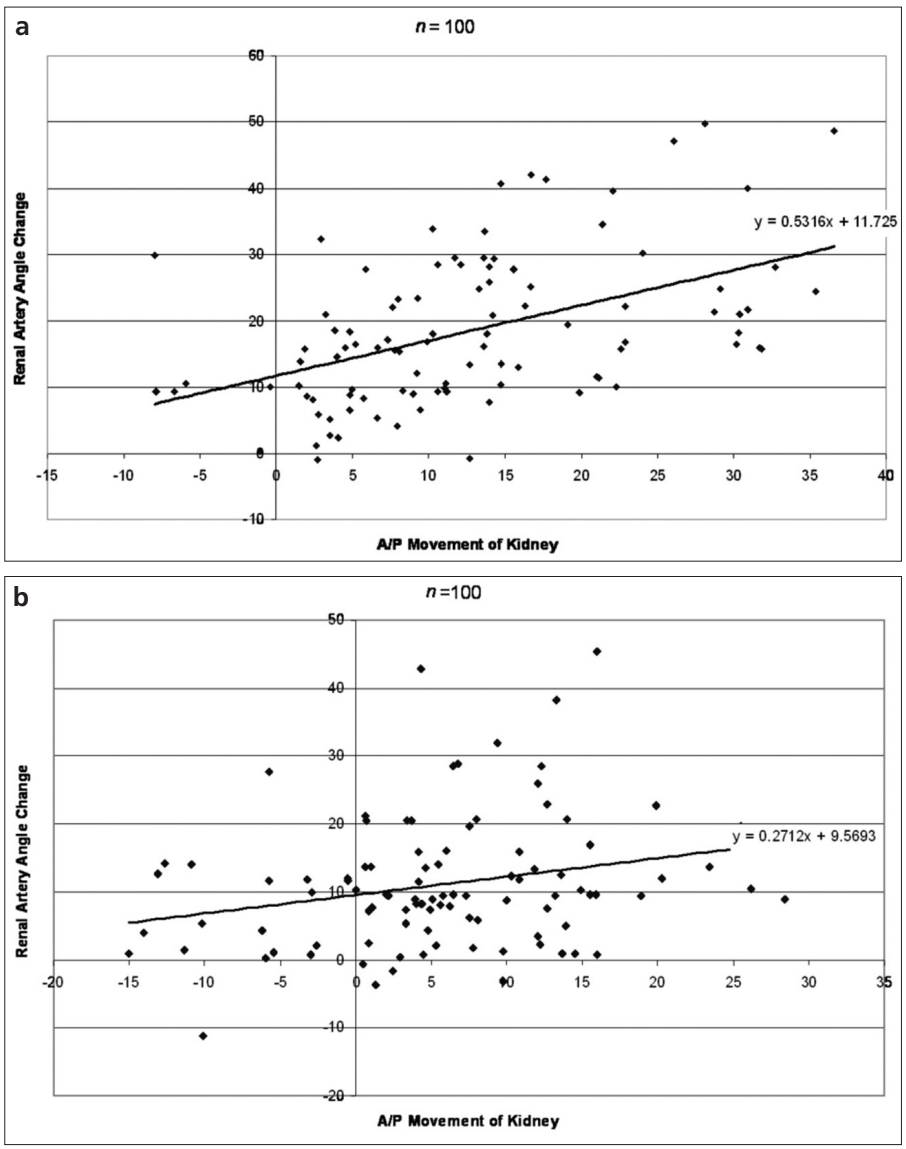

Figure 6. a, b. Scatter plot of the corresponding renal artery angle change and kidney mobility in the axial plane for the left **(a)** and right **(b)** sides.

axial plane (Table 2). The mean absolute angle change on either side and in either plane was 12.7°±9.6°. Mobility greater than one standard deviation above the mean (>22°) was present in 47 out of the 100 cases. Mobility greater than two standard deviations above the mean (>32°) was defined as extreme and was present in 14 out of the 100 cases.

Kidney-renal artery mobility correlation

In each patient, the axial plane renal artery angle change was plotted against the anteroposterior kidney movement for both the left and right side. The equations for the trend lines were y=0.4802x±12.05 for the left side and y=0.2506x±9.34 for the right side (Fig. 6). The same method was used to plot the coronal plane artery angle change against the cephalocaudal kidney mobility for both sides. The coronal plane trend line equations were y=0.2044x±3.45 for the left side and y=0.1245x±3.95 for the right side.

The Pearson correlation (*r*) was performed to evaluate the significance of the correlation between kidney mobility and the renal artery angle change and to evaluate the correlation between the movement of the right and left renal arteries within the same plane. In the axial plane, the correlation between the renal artery angle change and kidney movement was significant for both the left and right (r=0.44, $P < 0.01$ and r=0.22, $P = 0.03$, respectively). There was a correlation between the coronal plane artery angle change and cephalocaudal kidney movement on both sides, although this correlation was significant only on the left side (left: r=0.26, $P = 0.01$; right: r=0.18, $P = 0.08$). The correlation in angle change between the right and left renal arteries was significant in the axial plane but not in the coronal plane (axial r=0.2, $P = 0.04$; coronal r=0.11, $P = 0.28$). There was no correlation in renal artery movement between the axial and coronal planes on the same side (left: r=-0.13, $P = 0.33$; right: r=-0.07, $P = 0.46$). Therefore, the amount of arterial mobility in one plane did not predict the amount of movement in the other plane.

Male-female variability

There were significant male-female differences in left artery angle change and left kidney mobility, both in the

Table 2. Renal artery angle change (n=100 patients)

		Angle in prone position	Angle in supine position	Change in angle (Prone–supine)
Axial plane				
	Left renal artery	106°	88°	18° (range, -1° to 42°) $P < 0.01$
	Right renal artery	92°	84°	8° (range, -4 ° to 32°) $P < 0.01$
Coronal plane				
	Left renal artery	73°	68°	4° (range, -19° to 25°) $P < 0.01$
	Right renal artery	68°	60°	8° (range, -10° to 27°) $P < 0.01$

coronal plane ($P = 0.007$ and $P = 0.03$, respectively). All other measurements were similar between the sexes.

Measurement variability

The intra- and inter-observer CCC and *r* were both greater than 0.80 for kidney mobility on both sides and in both planes and for the left-sided axial renal artery angle change. The CCC and *r* values >0.80 indicated that these particular results were reliable. Lower measurement reproducibility was observed for the measured angle changes in the coronal plane on both sides and in the right renal artery angle change in the axial plane (Observer 1 left/right coronal and right axial: CCC=0.43/0.54 and 0.66, *r*=0.49/0.56 and 0.81, respectively; Observer 2 left/right coronal and right axial: CCC=0.63/0.67 and 0.46, *r*=0.64/0.71 and 0.46, respectively; inter-observer agreement left/right coronal: CCC=0.56/0.65, *r*=0.59/0.69, and right axial CCC=0.24, *r*=0.33).

Discussion

Renal movement had a direct small but statistically significant correlation with renal artery angle change on both sides in the axial plane. Axial plane direction changes in kidney position and renal artery angle were smaller in magnitude on the right side compared to the left side. This difference in mobility may be related to the right kidney's position caudal to the liver, which hinders the kidney from moving forward, and the right renal artery position posterior to the inferior vena cava (IVC), which prevents movement of the artery. Conversely, Suh et al. suggested that greater movement of the left renal artery could be due to its greater entanglement, creating fulcrum points along the vessel (Suh et al., presented at the 2007 ASME Summer Bioengineering Conference in Keystone, Colorado, USA). Consistent with these findings, stent fractures were found to be more frequent on the left by Robertson et al. (8) (left, 67%; right, 33%).

The relationship between kidney mobility and renal artery angle change was significant for the left side but was not significant on the right in the coronal plane. We postulate that the lack of correlation on the right is based on two anatomic factors. First, the IVC may have hindered right renal artery movement in the coronal direction when the kidney changed positions. Second, the renal arteries have a naturally occurring bend that is more acute on the right due to the renal artery's course behind the IVC (27). Our angle measurements were based only on the proximal segment of the artery and likely insufficiently captured the mobility or angle change of the distal portion of the artery. Therefore, a kidney movement in the cephalic direction will move the distal artery alone, without significantly affecting the proximal artery position or angle. In agreement with the results of a previous study, we found that the maximal coronal plane kidney displacement occurred on the right (27).

Our study had several limitations. One observer was used to make all of the CT measurements used for data analysis. This limitation was partially addressed by showing an intra- and inter-observer correlation greater than 0.80 for the majority of measurements. Our study did not evaluate movement that occurs during posture change from supine or prone to upright. However, CT scanning in the upright position was not feasible, and our aim was to establish a practical test that could identify patients with highly mobile arteries. Due to the measurement method, only proximal renal artery movement with respect to the aorta was evaluated, and distal bending was not assessed. However, because the majority of atherosclerotic disease, and therefore stenting, is localized to the proximal portion of the renal artery, this limitation may not necessarily hinder the usefulness of our results. All CT colonography exams in this study were performed without contrast and at a low radiation dose. While the use of contrast and a higher radiation dose may have resulted in superior image quality, the image resolution in this study was adequate to assess renal position and vasculature. Because the aim of our study was to evaluate both a practical and minimally invasive method to test for kidney mobility, the use of contrast or a higher radiation dose would have undermined the future applicability of our results. Finally, while the effect of respiration was not addressed in this study, previous studies have shown that respiratory motion has an effect on renal displacement (27–29). Although all patients were scanned using breath-hold after maximal inspiration in both the supine and prone positions, the prone position likely prevented the same amount of inspiration as in the supine position.

Our data support a direct relationship between kidney mobility and the change in the renal artery angle as viewed in multiple planes. Our results are consistent with those of a prior study and confirm the finding that kidney movement occurs with changes in body position (36). This movement is likely implicated in stent fracture (7–11). Additionally, inflammation and intimal hyperplasia caused by excessive stent movement may promote restenosis and thrombosis (17). In patients who develop stent failure or thrombosis, low-dose CT scans in varying positions may reveal if kidney mobility was an implicating factor. Knowledge of renal artery mobility and biomechanics may also be employed for stent design and in planning trans-renal aortic graft placement (37–39).

The current study provides a benchmark range of movement that can be used as a reference for comparison.

It is unknown what magnitude of renal artery angle change may be clinically significant. Our study had a wide range of measured renal artery angle changes; 47% of patients had an angle change greater than 22°, and 14% had a change of 32° or more. We suggest further study regarding kidney mobility in cases of stent intervention failure, which will lead to a more complete understanding of the factors involved in failure and improve future treatment options.

Conflict of interest disclosure

The authors declared no conflicts of interest.

References

1. Rammer M, Kramar R, Eber B. Atherosclerotic renal artery stenosis. Dtsch Med Wochenschr 2007; 132:2458–2462.
2. Ruchin PE, Baron DW, Wilson SH, Boland J, Muller DW, Roy PR. Long-term follow-up of renal artery stenting in an Australian population. Heart Lung Circ 2007; 16:79–84.
3. Bakker J, Beutler JJ, Elgersma OE, de Lange EE, de Kort GA, Beek FJ. Duplex ultrasonography in assessing restenosis of renal artery stents. Cardiovasc Intervent Radiol 1999; 22:475–480.
4. Leertouwer TC, Gussenhoven EJ, Bosch JL, et al. Stent placement for renal arterial stenosis: Where do we stand? A meta-analysis. Radiology 2000; 216:78–85.
5. Davies MG, Saad WE, Peden EK, Mohiuddin IT, Naoum JJ, Lumsden AB. The long-term outcomes of percutaneous therapy for renal artery fibromuscular dysplasia. J Vasc Surg 2008; 48:865–871.
6. Kane GC, Hambly N, Textor SC, Stanson AW, Garovic VD. Restenosis following percutaneous renal artery revascularization. Nephron Clin Pract 2007; 107:63–69.
7. Sahin S, Memis A, Parildar M, Oran I. Fracture of a renal artery stent due to mobile kidney. Cardiovasc Intervent Radiol 2005; 28:683–685.
8. Robertson SW, Jessup DB, Boero IJ, Cheng CP. Right renal artery in vivo stent fracture. J Vasc Interv Radiol 2008; 19:439–442.
9. Cohen DE. Re: Right renal artery in vivo stent fracture. J Vasc Interv Radiol 2008; 19:1391–1392.
10. Nallusamy A, Sundaram V, Abraham G, Mathew M, Das L. Recurrent hypertension from stent fracture. Kidney Int 2008; 73:1446.
11. Bessias N, Sfyroeras G, Moulakakis KG, Karakasis F, Ferentinou E, Andrikopoulos V. Renal artery thrombosis caused by stent fracture in a single kidney patient. J Endovasc Ther 2005; 12:516–520.
12. Sacks BA, Miller A, Gottlieb M. Fracture of an iliac artery Palmaz stent. J Vasc Intervent Radiol 1996; 7:53–55.
13. Rits J, van Herwaarden JA, Jahrome AK, Krievins D, Moll FL. The incidence of arterial stent fractures with exclusion of coronary, aortic, and non-arterial settings. Eur J Vasc Endovasc Surg 2008; 36:339–345.
14. Sriram PV, Ramakrishnan A, Rao GV, et al. Spontaneous fracture of a biliary self-expanding metal stent. Endoscopy 2008; 36:1035–1036.
15. Scheinert D, Scheinert S, Sax J, et al. Prevalence and clinical impact of stent fractures after femoropopliteal stenting. J Am Coll Cardiol 2005; 45:312–315.
16. Allie DE, Hebert CJ, Ricis RT, Walker GCM. Nitinol stent fractures in the SFA. Endovasc Today 2004; 7:22–34.
17. van Lankeren W, Gussenhoven EJ, van Kints MJ, et al. Stent remodeling contributes to femoropopliteal artery restenosis: an intravascular ultrasound study. J Vasc Surg 1997; 25:753–756.
18. Farb A, Sangiorgi G, Carter AJ, Walley VM,et al. Pathology of acute and chronic coronary stenting in humans. Circulation 1999; 99:44–52.
19. Feldman LJ, Aguirre L, Ziol M, Bridou JP, Nevo N,et al. Interleukin-10 inhibits intimal hyperplasia after angioplasty or stent implantation in hypercholesterolemic rabbits. Circulation 2000; 101:908–916.
20. Welt FG, Rogers C. Inflammation and restenosis in the stent era. Arterioscler Thromb Vasc Biol 2002; 22:1769–1776.
21. Indolfi C, Mongiardo A, Curcio A, Torella D. Molecular mechanisms of in-stent restenosis and approach to therapy with eluting stents. Trends Cardiovasc Med 2003; 13:142–148.
22. Edelman ER, Rogers C. Pathobiologic responses to stenting. Am J Cardiol 1998; 81:4E–6E.
23. Painter JA, Mintz GS, Wong SC, et al. Serial intravascular ultrasound studies fail to show evidence of chronic Palmaz-Schak stent recoil. Am J of Cardiol 1995; 75:398–400.
24. Farb A, Burke AP, Kolodgie FD, Virmani R. Pathological mechanisms of fatal late coronary stent thrombosis in humans. Circulation 2003; 108:1701–1706.
25. Khosla S, Shaw D, McCarthy N, et al. Mechanism of restenosis following stenting of renal arteries with nonarticulated Palmaz stents. J Am Coll Cardiol 1996; 27:111A.
26. Kuntz RE, Baim DS. Prevention of coronary restenosis: the evolving evidence base for radiation therapy. Circulation 2000; 101:2130–2133.
27. Draney MT, Zarins CK, Taylor CA. Three-dimensional analysis of renal artery bending motion during respiration. J Endovasc Ther 2005; 12:380–386.
28. Schwartz LH, Richaud J, Buffat L, Touboul E, Schlienger M. Kidney mobility during respiration. Radiother Oncol 1994; 32:84–86.
29. van Sörnsen de Koste JR, Senan S, Kleynen CE, Slotman BJ, Lagerwaard FJ. Renal mobility during uncoached quiet respiration: an analysis of 4DCT scans. Int J Radiat Oncol Biol Phys 2006; 64:799–803.
30. Pump B, Talleruphuus U, Christensen NJ, Warberg J, Norsk P. Effects of supine, prone, and lateral positions on cardiovascular and renal variables in humans. Am J Physiol Regul Integr Comp Physiol 2002; 28:174–180.
31. Norsk P. Gravitational stress and volume regulation. Clin. Physiol 1992; 12:505-526.
32. Schaefer WM, Lipke CS, Kuhl HP, et al. Prone versus supine patient positioning during gated 99mTc-sestamibi SPECT: effect on left ventricular volumes, ejection fraction, and heart rate. J Nucl Med 2004; 45:2016–2020.
33. Lin ZY, Dai CY, Chang WY, et al. Influence of postural change on intrarenal arteriaresistive index measurement. Abdom Imaging 2002; 27:626–628.
34. Dalal PG, Murray D, Feng A, Molter D, McAllister J. Upper airway dimensions in children using rigid video-bronchoscopy and a computer software: description of a measurement technique. Paediatr Anaesth 2008; 18:645–653.
35. Lorenzon M, Zuiani C, Londero V, Linda A, Furlan A, Bazzacchi M. Assessment of breast cancer response to neoadjuvant chemotherapy: Is volumetric MRI a reliable tool? Eur J Radiol 2009; 71:82-88.
36. Reiff JE, Werner-Wasik M, Valicenti RK, Huq MS. Changes in the size and location of kidneys from supine to standing positions and the implications for block placement during total body irradiation. Int J Radiat Oncol Biol Phys 1999; 45:447–449.
37. Ju F, Xia Z, Zhou C. Repeated unit cell (RUC) approach for pure bending analysis of coronary stents. Comput Methods Biomech Biomed Engin 2008; 11:419–431.
38. Harewood FJ, McHugh PE. Modeling of size dependent failure in cardiovascular stent struts under tension and bending. Ann Biomed Eng 2007; 35:1539–1553.
39. Muhs BE, Vincken KL, Teutelink A, et al. Dynamic cine-computed tomography angiography imaging of standard and fenestrated endografts: differing effects on renal artery motion. Vasc Endovascular Surg 2008; 42:25–31.